

XAFS spectroscopy at 4th generation synchrotron radiation sources

Opportunities and challenges

Edmund Welter

Hamburg/Melbourne, 16.06.2021

Agenda

01 Ultra low emittance storage rings

- The PETRA IV project as example
- Photon beam properties
- Brilliance / coherence / focusing

02 "Classical" XAFS spectroscopy

- Which properties are important for (XAFS) spectroscopy?
- Detectors
- Beam homogeneity

03 Beyond classical XAFS spectroscopy

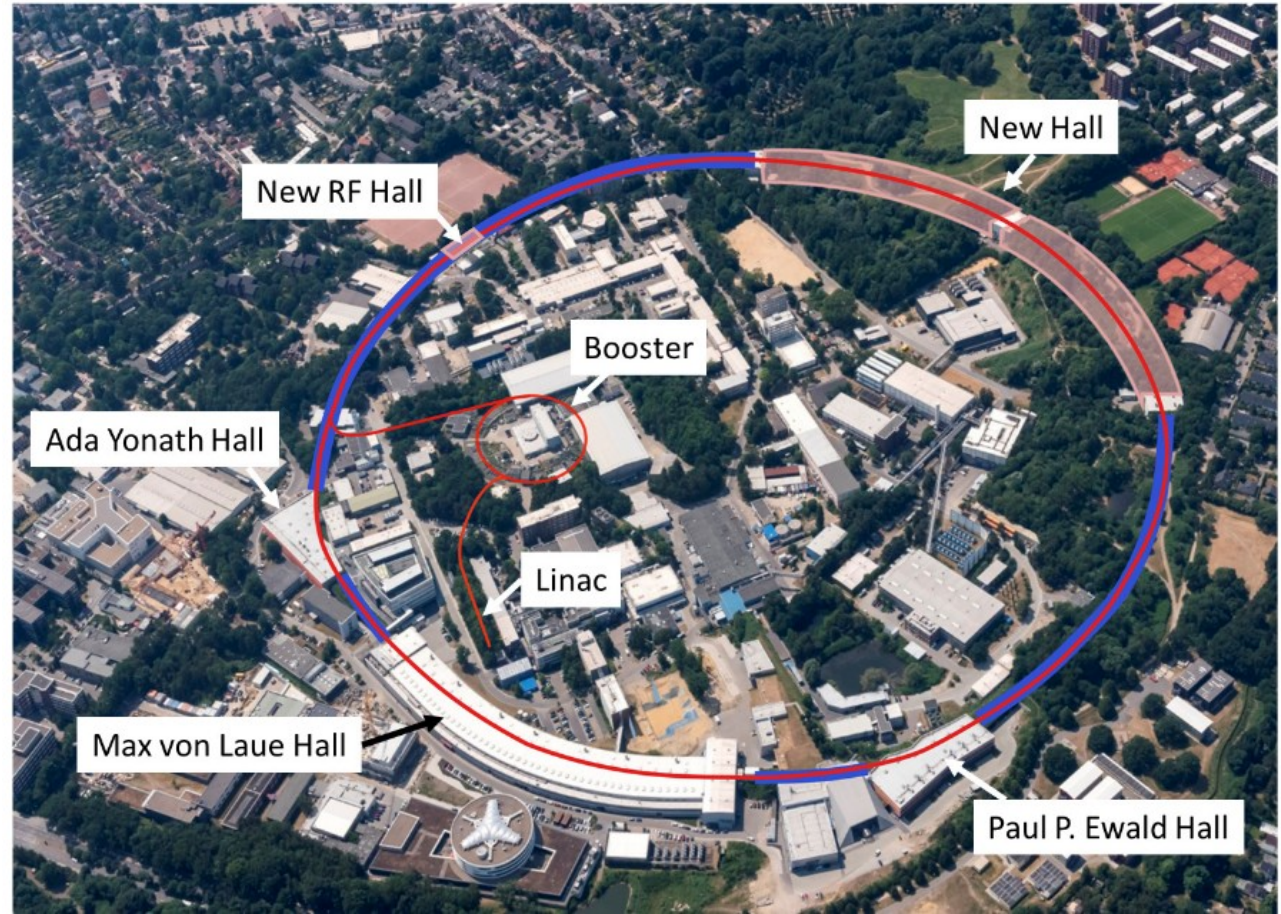
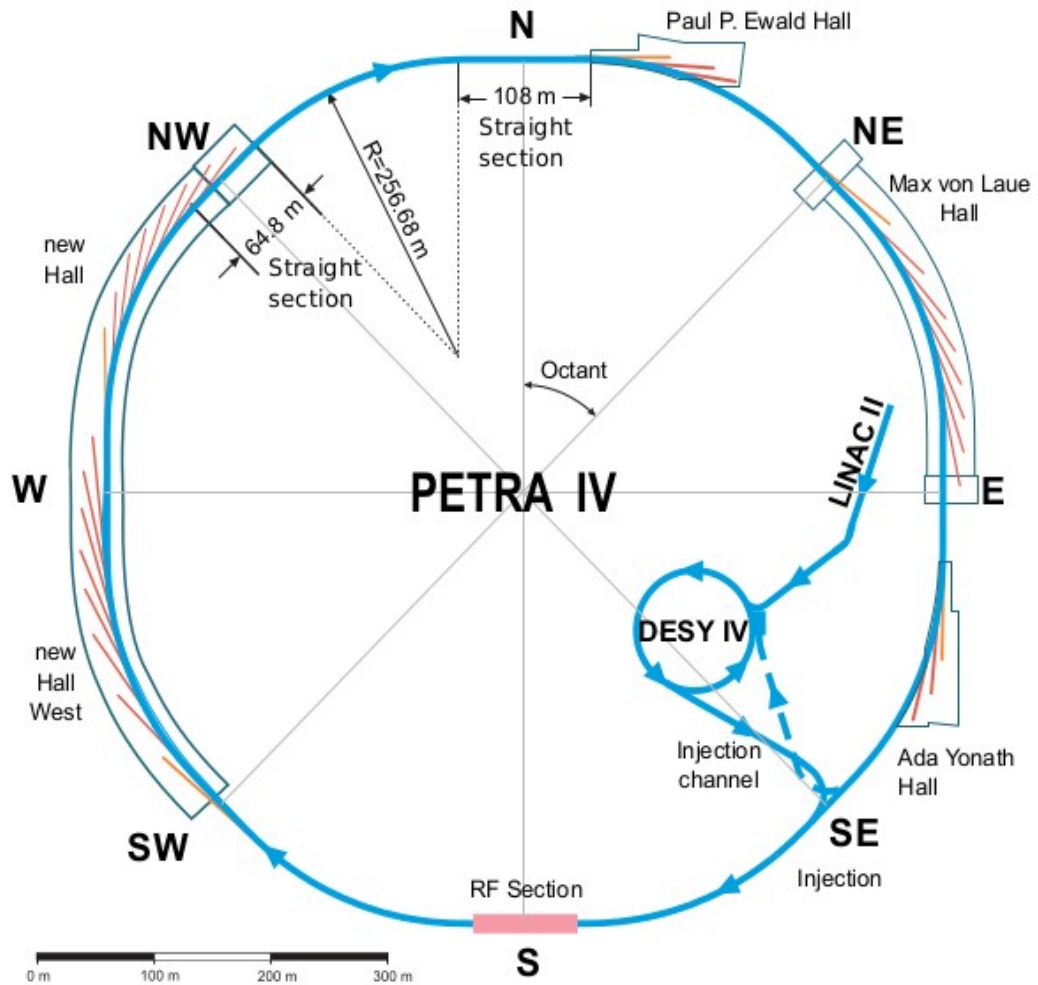
- High brilliance applications
 - μ -XAFS
 - XAFS tomography
- Coherence applications
 - XAFS-Ptychography

04 Summary

- Prospects for classical XAFS
- Prospects for high brilliance/coherence requiring methods

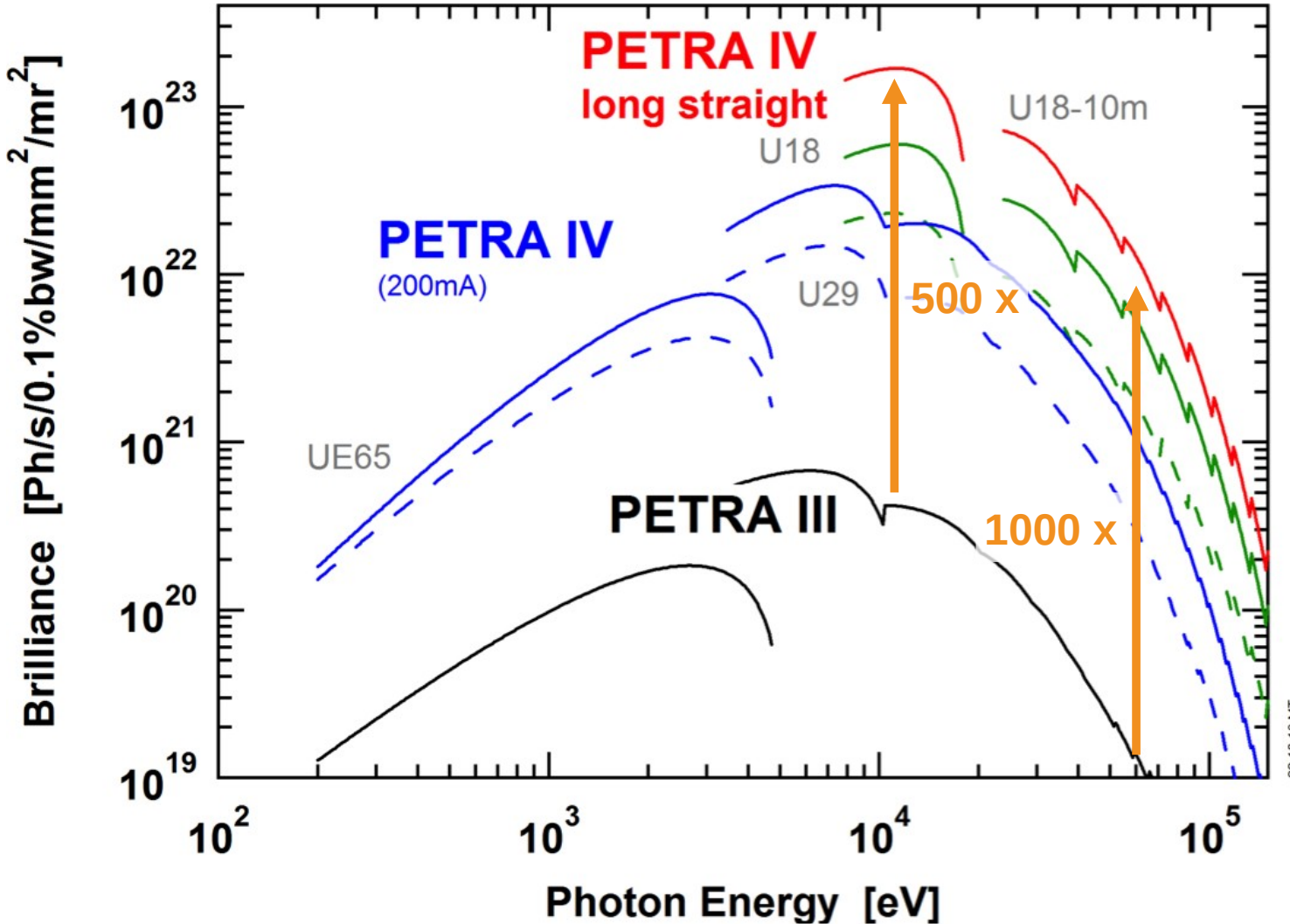
PETRA IV

Conversion of PETRA into a diffraction limited storage ring



PETRA IV

Brilliance



Based on current reference lattice:

> emittance:

→ coherence mode: 20 x 2 pmrad²

→ timing mode: 50 x 5 pmrad²

> undulators: 5 m, 10 m

> optimised beta (in 10 m section): 2 x 2 m²

> ring current: 200 mA

Brilliance increase by

→ 500 x (hard X-rays)

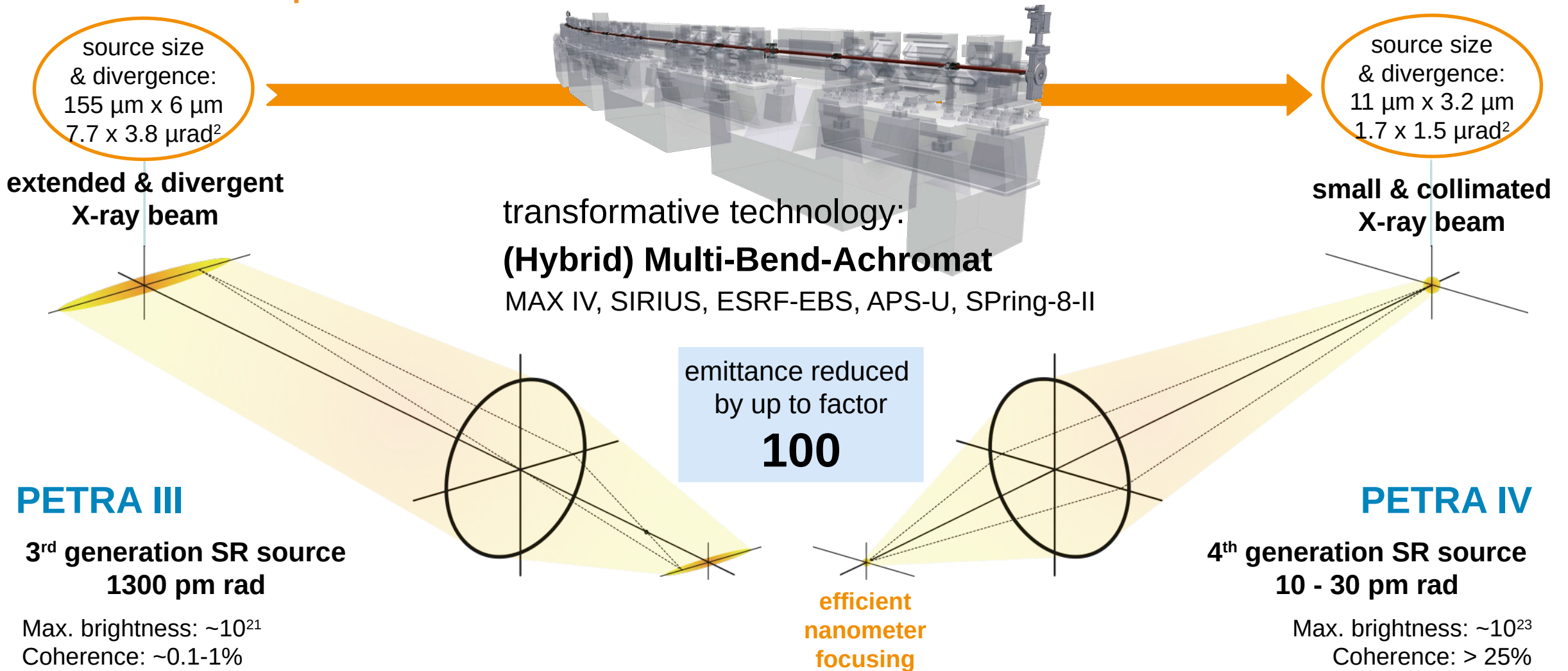
→ 1000 x (high-energy X-rays)

PETRA IV brilliance at 100 keV
same as for 10 keV at PETRA III today!!

C. G. Schroer, et al., JSR **25**, 1277 (2018).

Ultra Low Emittance Storage Rings

PETRA IV for example



Brilliance and coherent flux

Brilliance:

Flux per phase-space volume

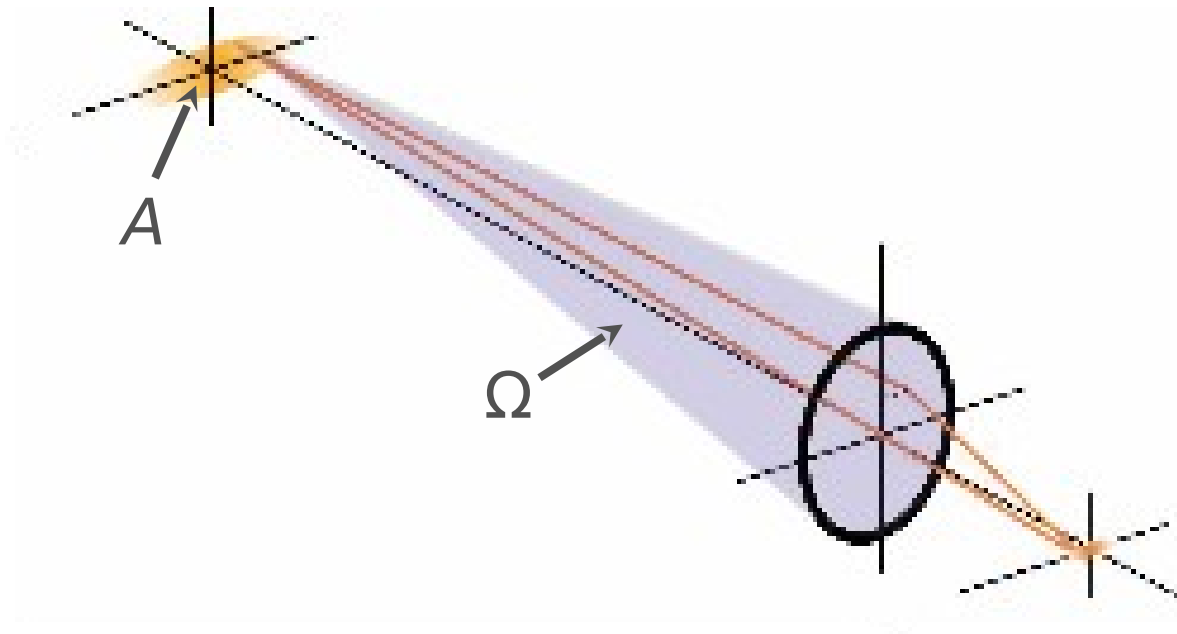
$$B_{\text{sp}} = \frac{F}{\Omega \cdot A \cdot \Delta E / E}$$

Coherent flux:

$$F_c \propto B_{\text{sp}} \cdot \lambda^2 \cdot \frac{\Delta E}{E}$$

Improvements in Brilliance allow:

- > faster measurements (time resolution)
- > nano-imaging (spatial resolution)
- > spectroscopy (energy resolution)



Coherent flux

Coherent flux for a given bandwidth:

$$F_c = F_0 \cdot \frac{l_{c_h}}{2\Sigma_h} \cdot \frac{l_{c_v}}{2\Sigma_v} = F_0 \cdot \frac{\lambda^2}{(4\pi)^2 \sigma_{T_h} \sigma'_{T_h} \sigma_{T_v} \sigma'_{T_v}} = Br \cdot \left(\frac{\lambda}{2}\right)^2$$

The total flux F_0 depends on **storage ring energy** and **undulator**

- F_0 will not change with improved emittance as long as storage ring energy remains unchanged (improvements using better (longer) undulators)
- Experiments that do not require focusing or coherence will not profit much!

Up to 10 keV:

> diffraction limited beam: whole beam can be focused (lateral coherence)

High-energy x-rays:

- > diffraction limit can not be reached
- > full gain in coherent (focused) flux (~ 100 x).

PETRA IV:

Ultimate 3D Microscope for Physical, Chemical and Biological Processes

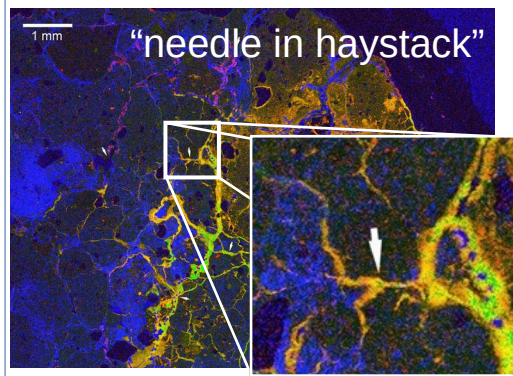
Hard X-ray beam (nearly) diffraction limited:

→ Nanoprobes: focus nearly full flux to nanobeam

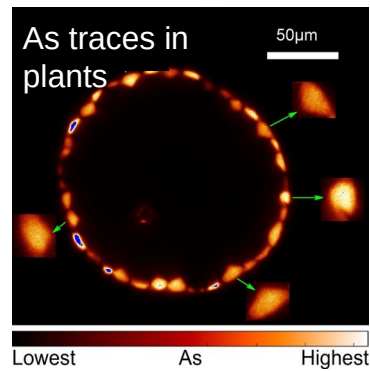
- > up to **500 x faster** (movies rather than static images)
- > up to **20 x better sensitivity** (signal-to-noise ratio)
- > up to **500 x larger field of view** or sample volumes (“needle in haystack” problem)

→ Coherent imaging:

- > 4 to 5 orders of magnitude higher coherent flux density



CSIRO: gold deposit in clay



S. Mishra et al, J Exp Bot **67**, 4639 (2016).

New, unique properties:

→ Local quantitative measurements with all X-ray analytical techniques!

→ Flux-hungry techniques go nano!

- > inelastic X-ray scattering,
- > nuclear resonance scattering
- > resonant magnetic hard X-ray scattering

→ High-energy X-ray techniques go nano!

- > Compton scattering
- > Pair distribution function, ...

→ Spatial resolution of coherent imaging:

→ all spatial dimensions down to < 1 nm!

- > ptychographic imaging

PETRA IV:

Ultimate 3D Microscope for Physical, Chemical and Biological Processes

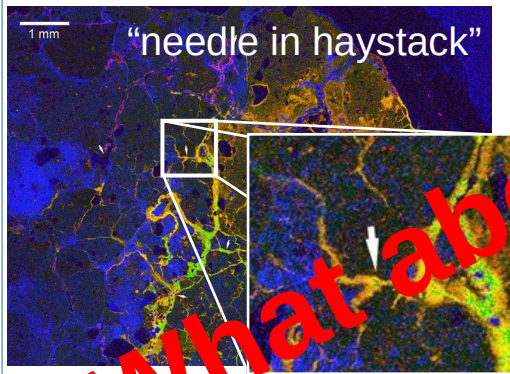
Hard X-ray beam (nearly) diffraction limited:

→ Nanoprobes: focus nearly full flux to nanobeam

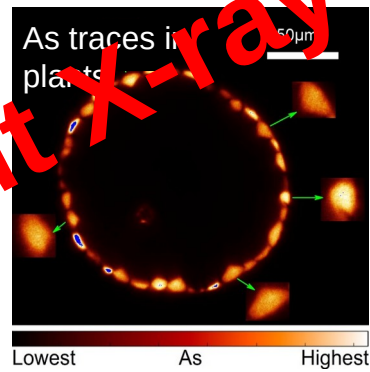
- > up to **500 x faster** (movies rather than static images)
- > up to **20 x better sensitivity** (signal-to-noise ratio)
- > up to **500 x larger field of view** or sample volumes (“needle in haystack” problem)

→ Coherent imaging:

- > 4 to 5 orders of magnitude higher coherent flux density



CSIRO. gold deposit in clay



S. Mishra et al, J Exp Bot **67**, 4639 (2016).

New, unique properties:

→ Local quantitative measurements with all X-ray analytical techniques!

→ Flux-hungry techniques go nano!

- > inelastic X-ray scattering,
- > nuclear resonance scattering
- > resonant magnetic hard X-ray scattering

→ High-energy X-ray techniques go nano!

- > Compton scattering
- > Pair distribution function, ...

→ Spatial resolution of coherent imaging:

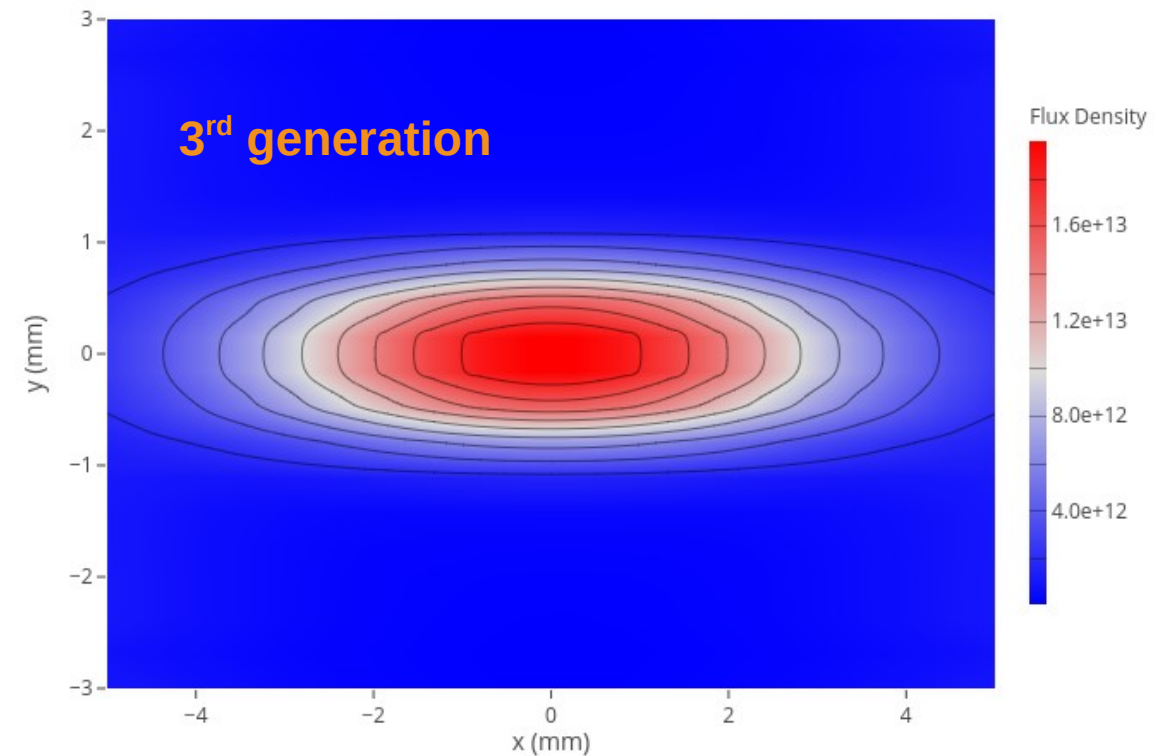
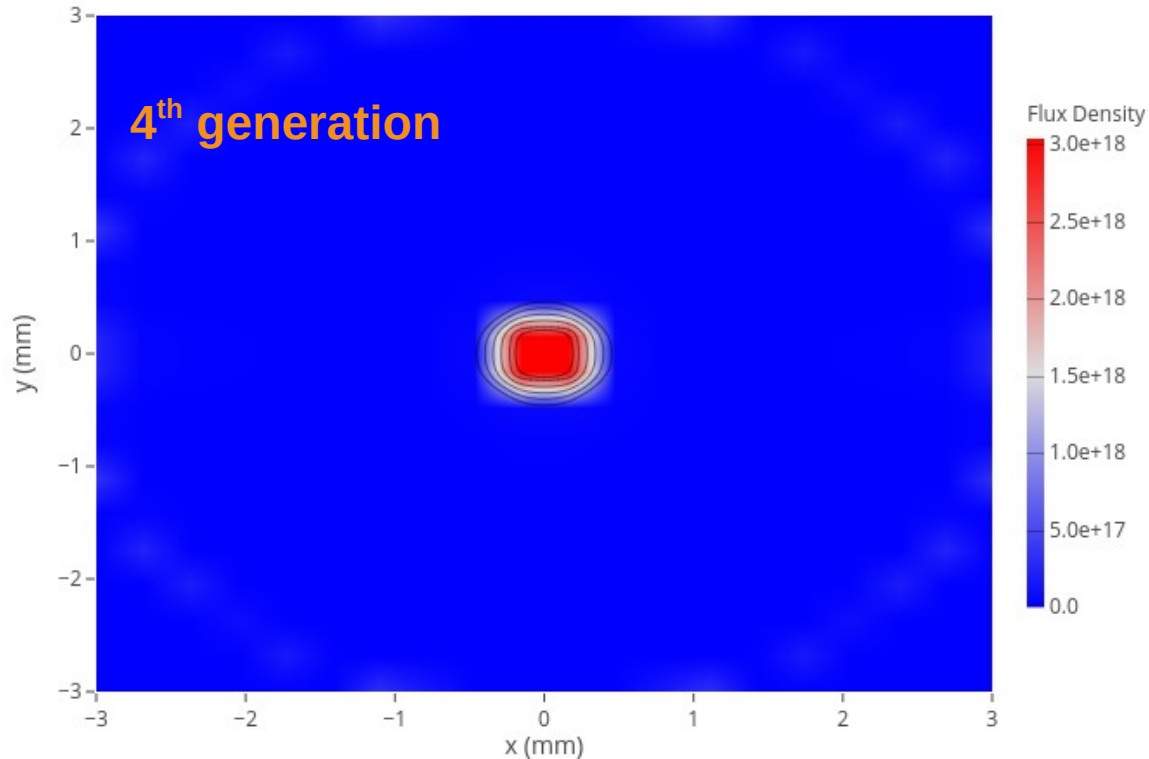
→ all spatial dimensions down to < 1 nm!

- > ptychographic imaging

Beam properties at the sample

Flux density

80 m from a 5 m long undulator



Undulator: U33, 150 periods, 3rd harmonic
Storage ring: PETRA IV, 200 mA, 1600 bunches

Undulator: U33, 59 periods, 3rd harmonic
Storage ring: PETRA III, 100 mA, 480 bunches

Calculations done using SPECTRA 11, Tanaka T and Kitamura H 2001 J. Synchrotron Rad.8 1221

Flux through pinhole

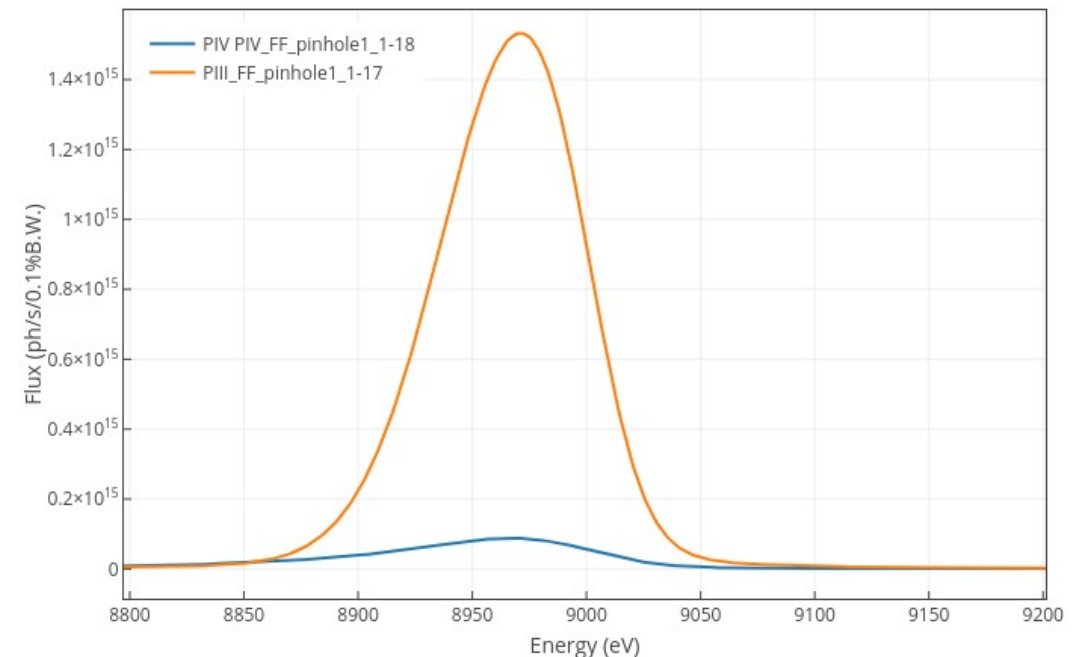
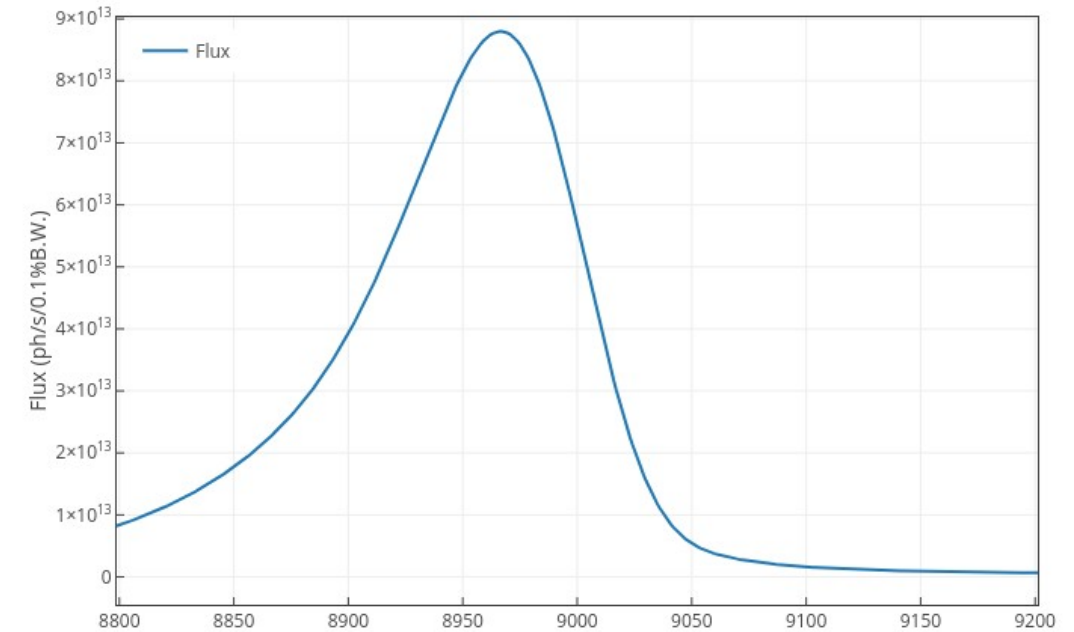
80 m from source

PETRA III

- 5 m U33
- Nat. emittance: 1.01 nmrad, 1 % coupling
- Ring current: 100 mA, 480 bunches
- 6 GeV
- 3rd harmonic

PETRA IV

- 2 m U33
- Nat. emittance: 12 pmrad, 20 % coupling
- ring current: 200 mA, 1600 bunches
- 6 GeV
- 3rd harmonic



Ray tracing through a moderately focused beamline

P64 as an example

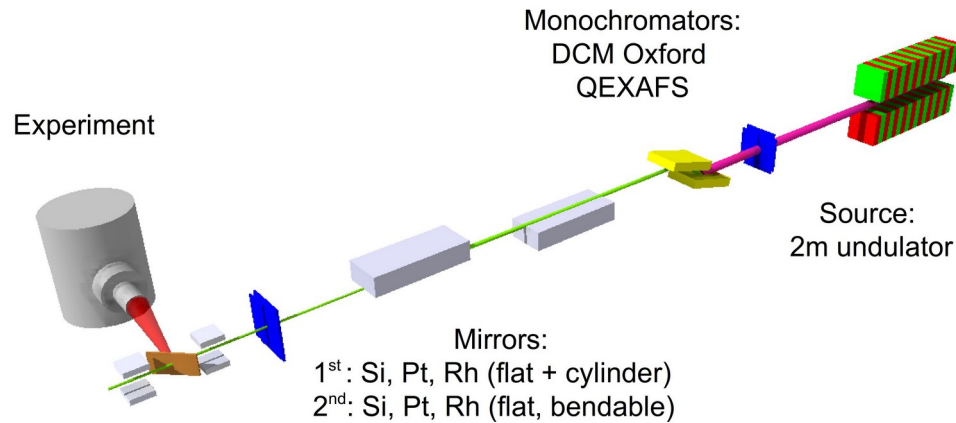


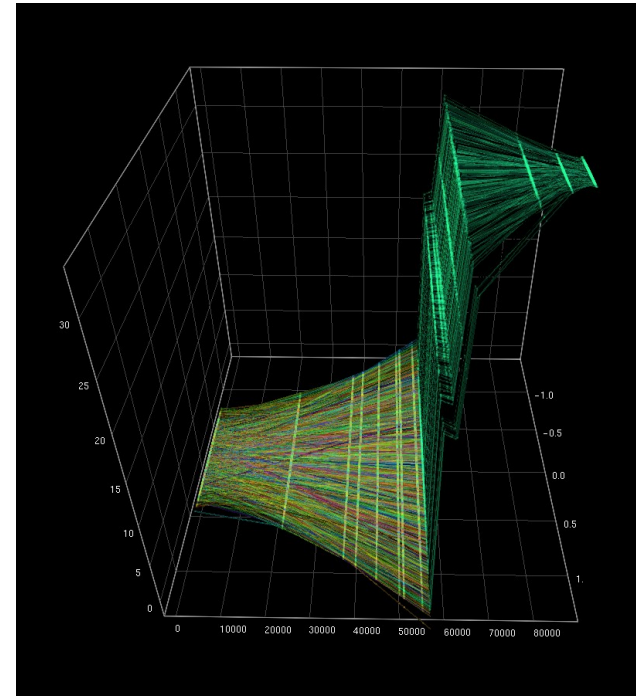
TABLE I. Distances of optical components from the source (middle of undulator).

| Component | Slit I (v) | Slit II (vxh) | Filter | Shutter | Q-Mono | DCM | Mirror I | Mirror II | Slit III (vxh) | Sample |
|------------|------------|---------------|--------|---------|--------|------|----------|-----------|----------------|--------|
| Distance/m | 37.1 | 44.8 | 45.6 | 48.9 | 52.4 | 56.6 | 58.7 | 60.5 | 87 | 87.2 |

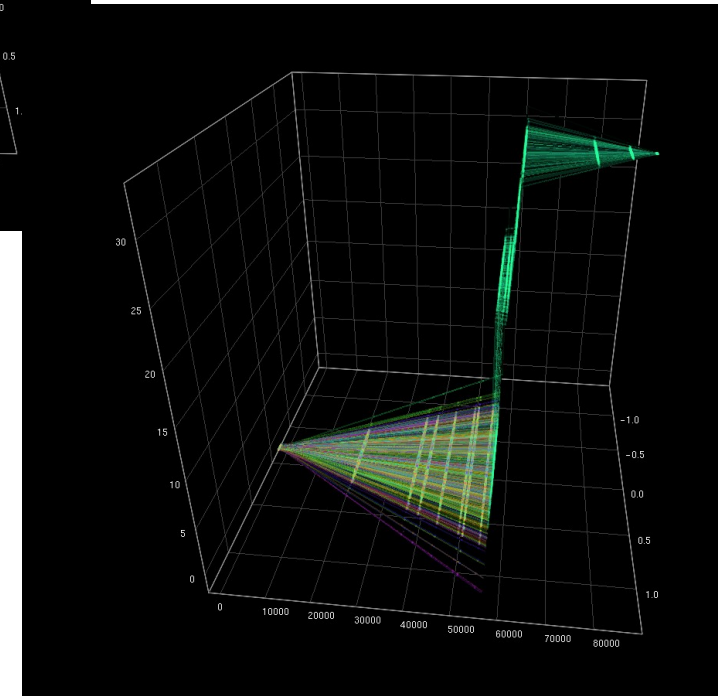
From W.A. Caliebe, AIP Conference Proceedings 2054, 060031 (2019);
<https://doi.org/10.1063/1.5084662>

Ray tracing done with xrt 1.3.5

K. Klementiev and R. Chernikov, "Powerful scriptable ray tracing package xrt", Proc. SPIE 9209, Advances in Computational Methods for X-Ray Optics III, 92090A; doi:10.1117/12.2061400



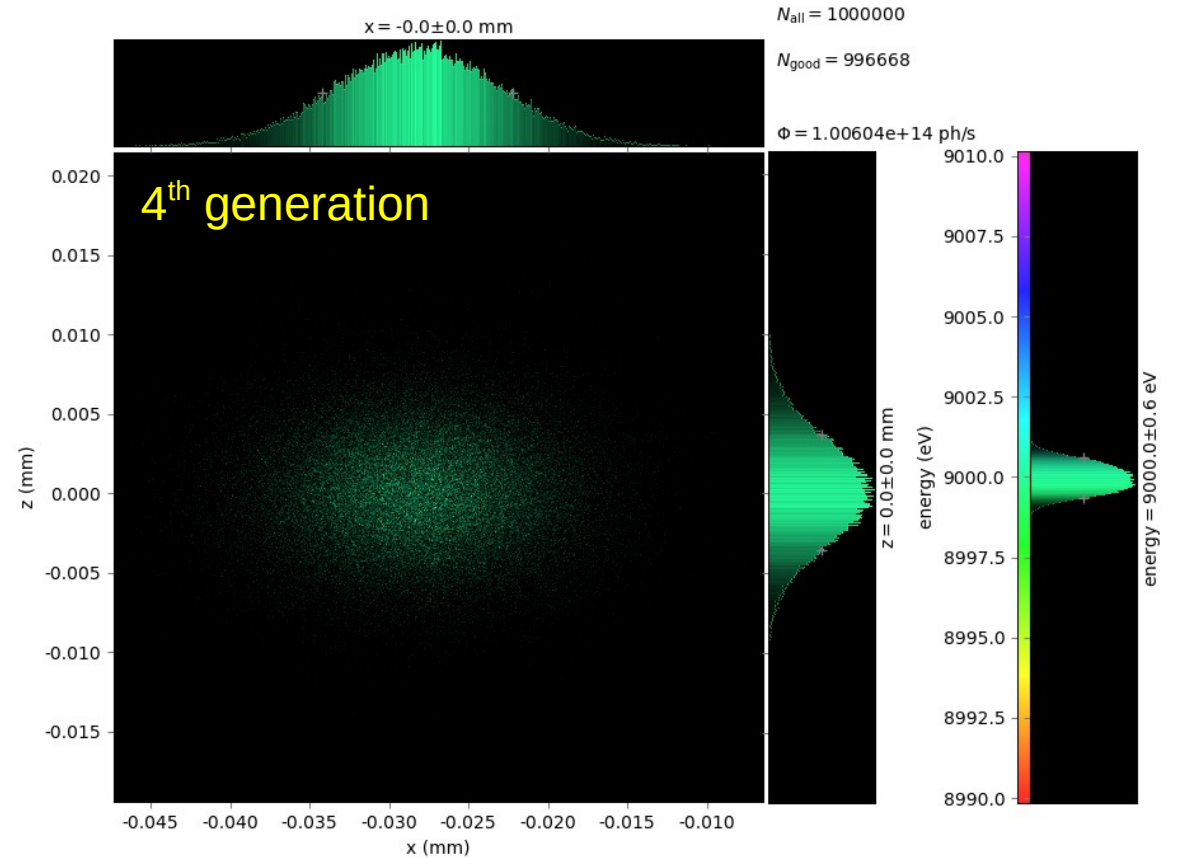
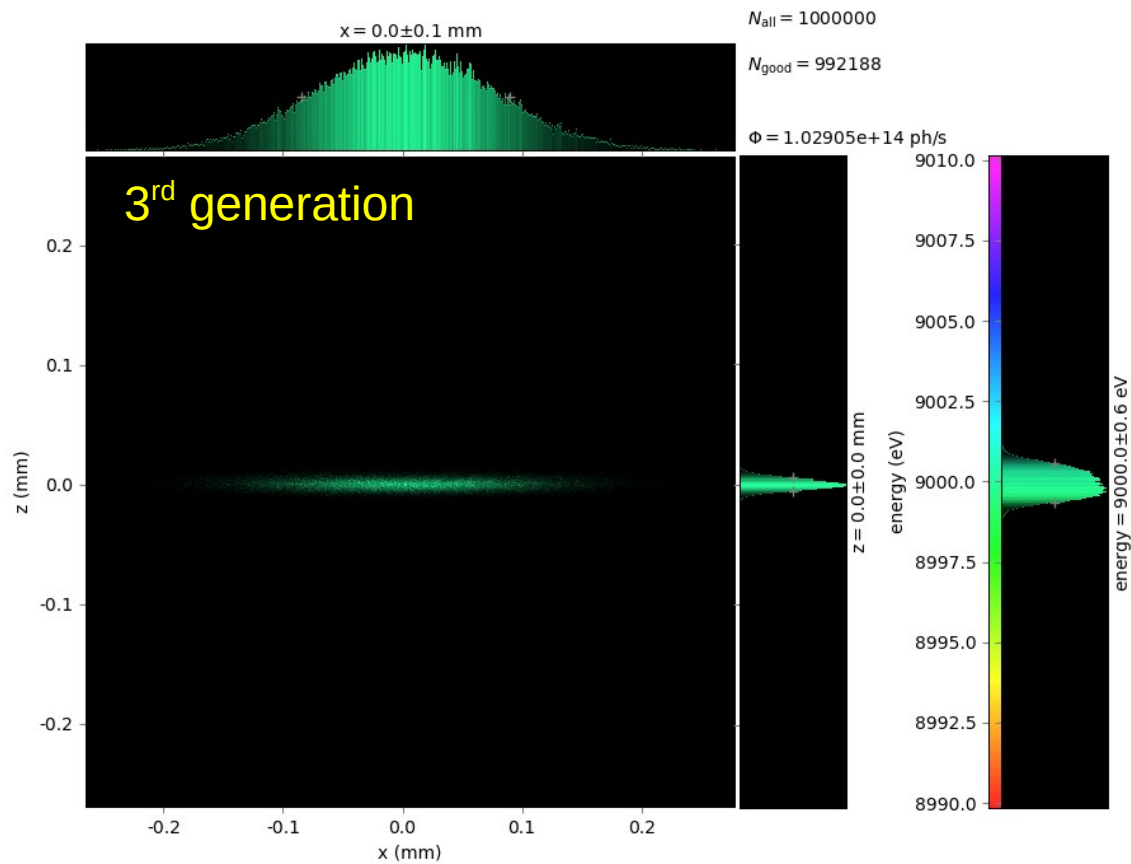
PETRA III



PETRA IV

Footprint 80 m from source

Focused beam 80 m from source



Observe the different scaling!

Classical XAFS spectroscopy

“Classical” X-ray absorption spectroscopy

The Swiss knife in catalysis...

Requires:

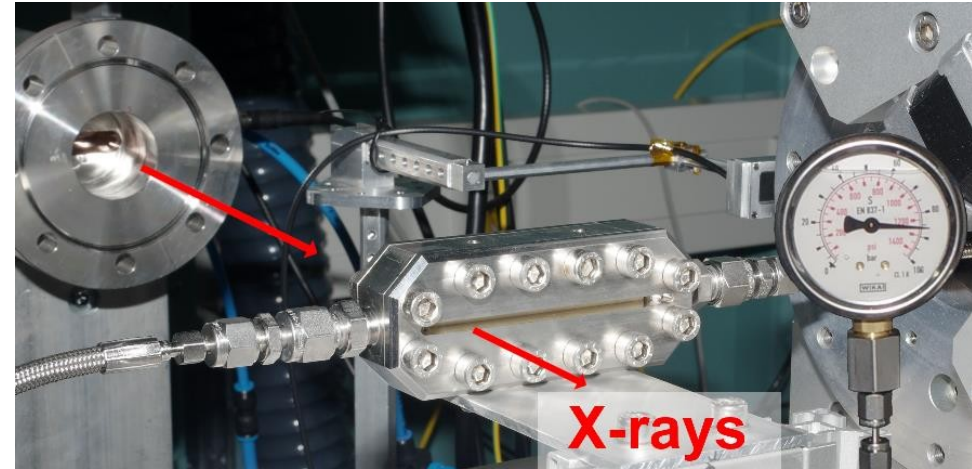
- mm² sized beam
 - Homogeneous and incoherent beam
 - Monochromatic flux: $> 10^9 \text{ s}^{-1}$
- => Ideal source: Bending magnet or short wiggler

Methods:

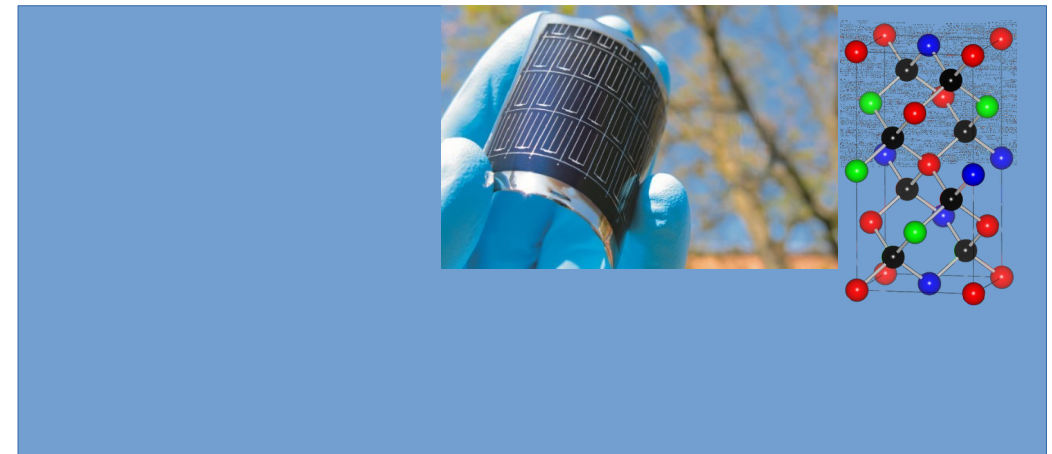
- XANES, EXAFS (Q-EXAFS)

Applications:

- In-situ experiments
 - Catalysis, Batteries...
- ex-situ
 - Geochemistry, material science, solid state physics...



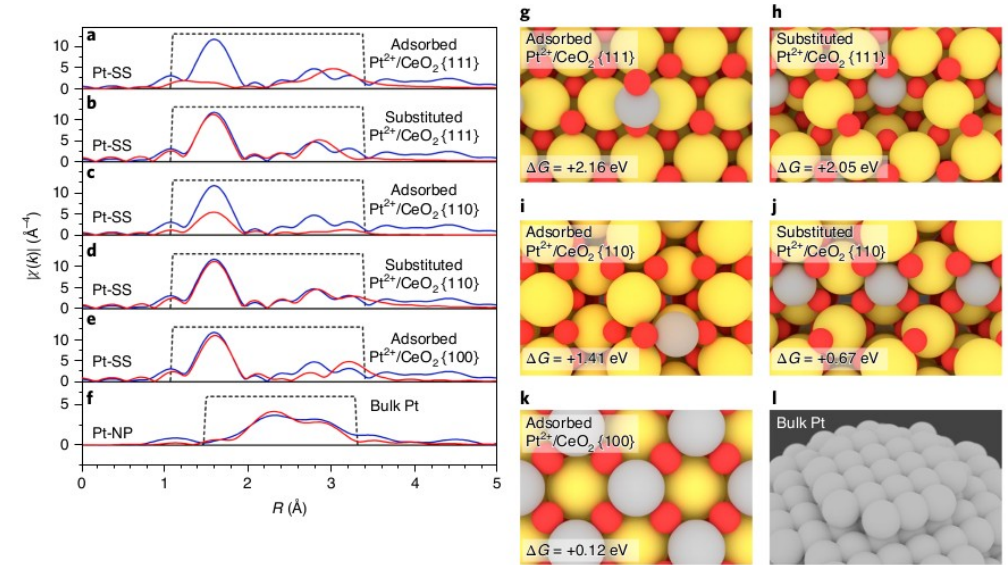
In situ reactor cell for operando XAS studies of direct synthesis of hydrogen peroxide at high pressure.



A “typical” XAFS experiment

Bulk XAFS with mm sized beam

- Use XANES and mainly EXAFS as analytical method
- In-situ/operando experiment
- XAFS as part of a suite of analytical methods
- XAFS results often decisive for the understanding of the structure of the system
- In high demand (High overbooking)



Fits of EXAFS spectra (left) of different structures found by DFT calculations (right) to the experimental spectrum of the active catalyst.

F. Maurer et al., *Nature cat.*, 3, 824-833 (2020)

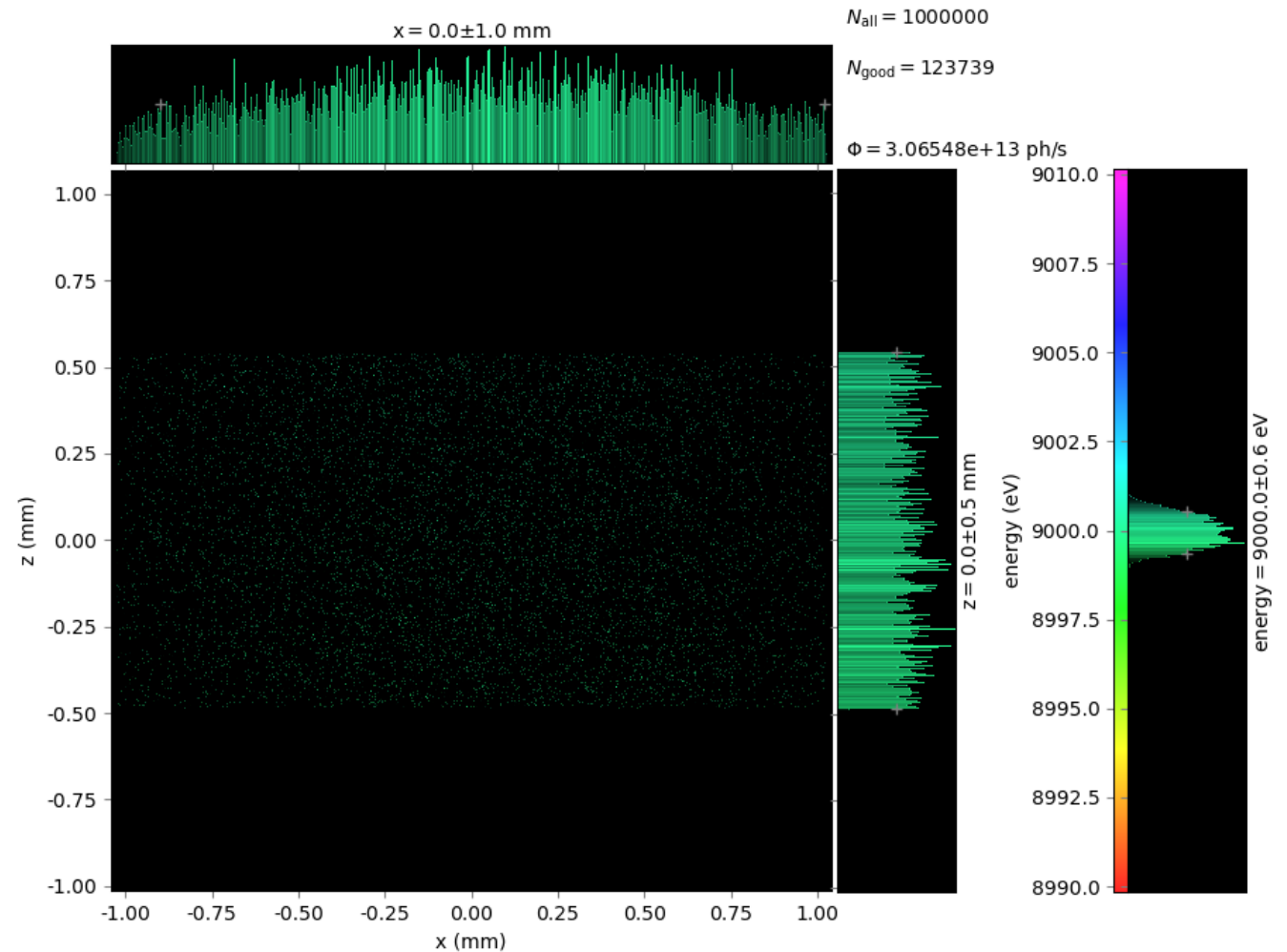
An undulator beamline for bulk XAFS

Ray tracing parameter:

- 15 period U33
- Sample 80 m from source
- 2 plane mirrors for higher harmonic rejection
- Si 111 (and 311) DCM
- Final slit $0.5 \times 1 \text{ mm}^2$ (v*h)
- Tuned to 9000 eV

Today (P65):

- 11 period U33
- Beamspace $0.5 \times 1.5 \text{ mm}^2$ (v*h)
- Monochromatic flux $\sim 10^{12} \text{ s}^{-1}$



=> Comparable beamspace, x10 increased flux (density)

An undulator beamline for bulk XAFS

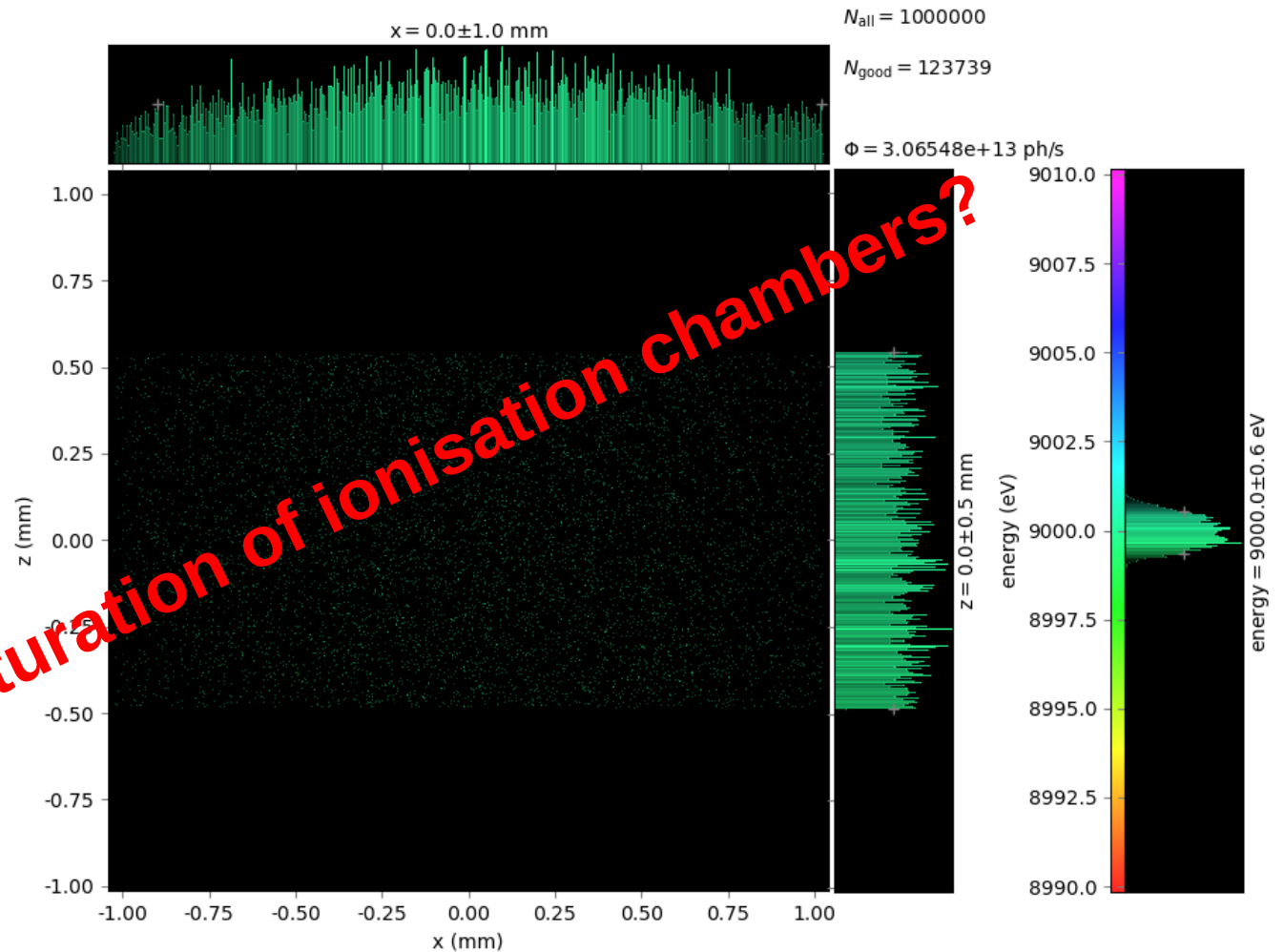
Ray tracing parameter:

- 15 period U33
- Sample 80 m from source
- 2 plane mirrors for higher harmonic rejection
- Si 111 (and 311) DCM
- Final slit 0.5*1 mm² (v*h)
- Tuned to 9000 eV

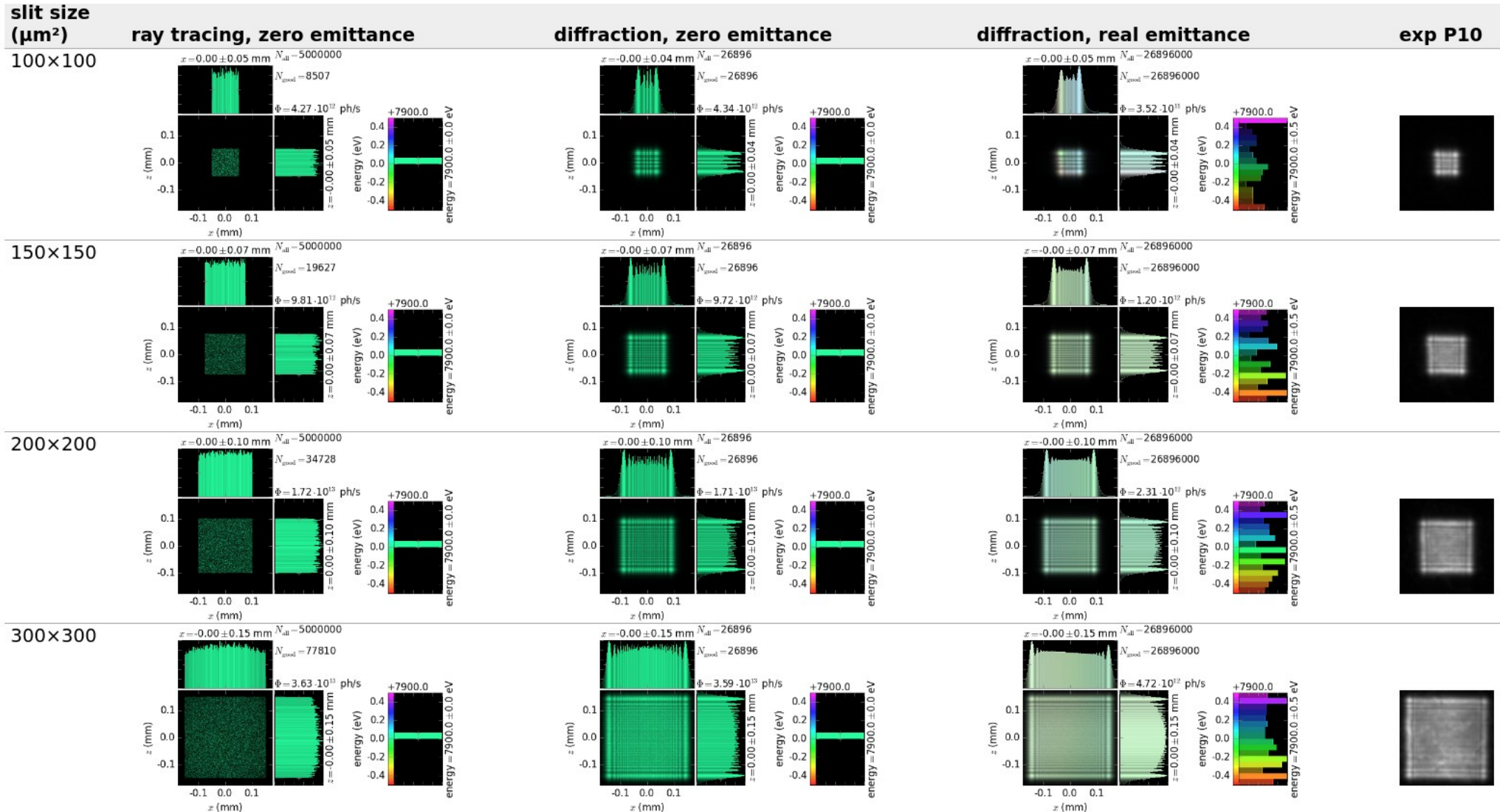
Today (P65):

- 11 period U33
- Beamspace 0.5*1.5 mm² (v*h)
- Monochromatic flux $\sim 10^{12}$ s⁻¹

Radiation damage, saturation of ionisation chambers?



Diffraction by slits

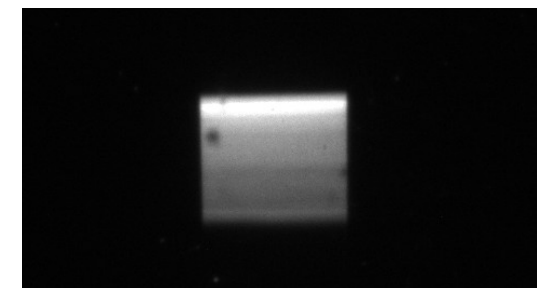
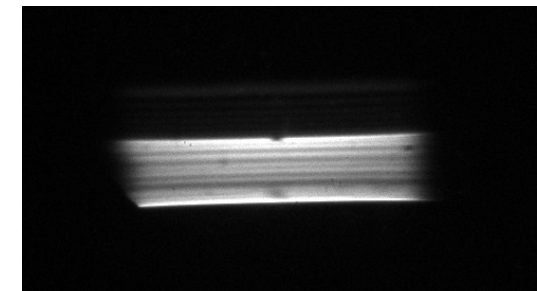
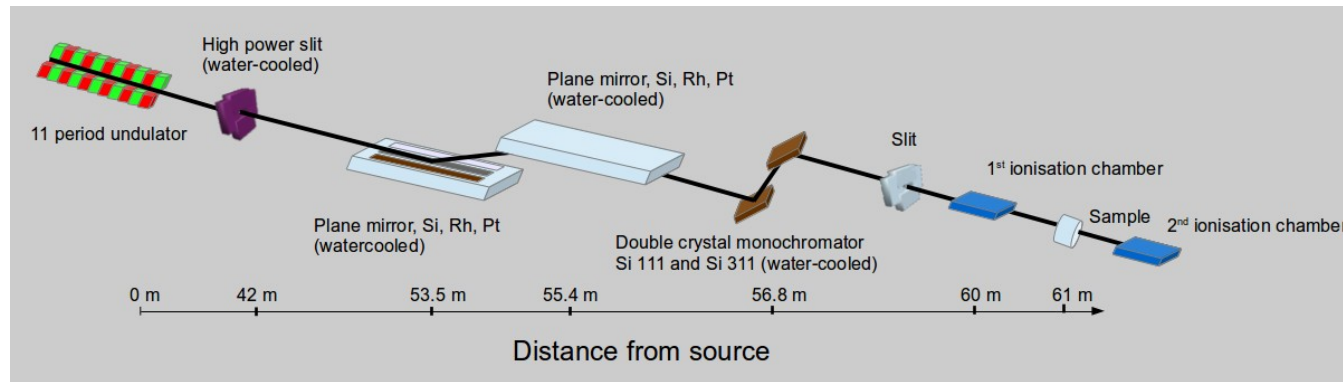
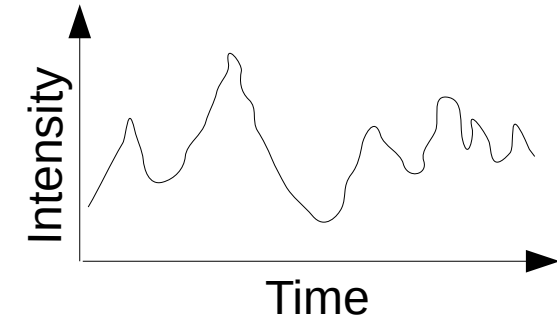
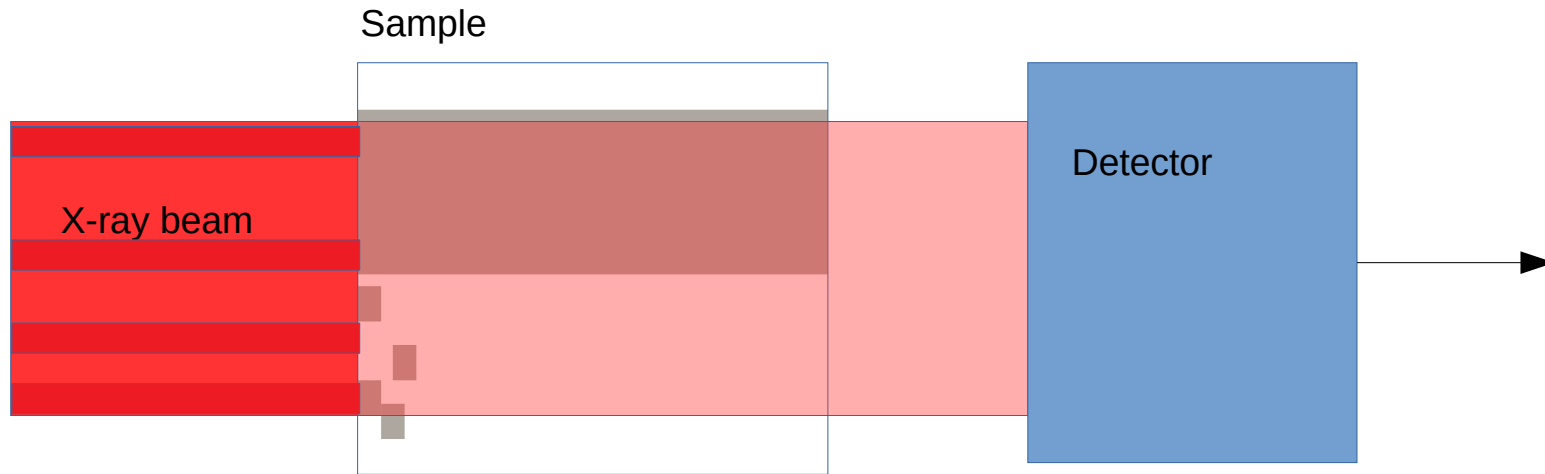


Xrt calculations of undulator beam diffraction at rectangular slits by K. Klementiev and R. Chernikov.

<https://xrt.readthedocs.io/gallery3.html>

Calculated and measured diffraction by rectangular slits, exp. from PETRA III beamline P10 (A. Zozulya and M. Sprung, 2010, unpublished)

Inhomogeneous beam hits inhomogeneous sample



Beam at sample position (P65)

Long distances => Small movements of beam position unavoidable...
=> **NOISE!**

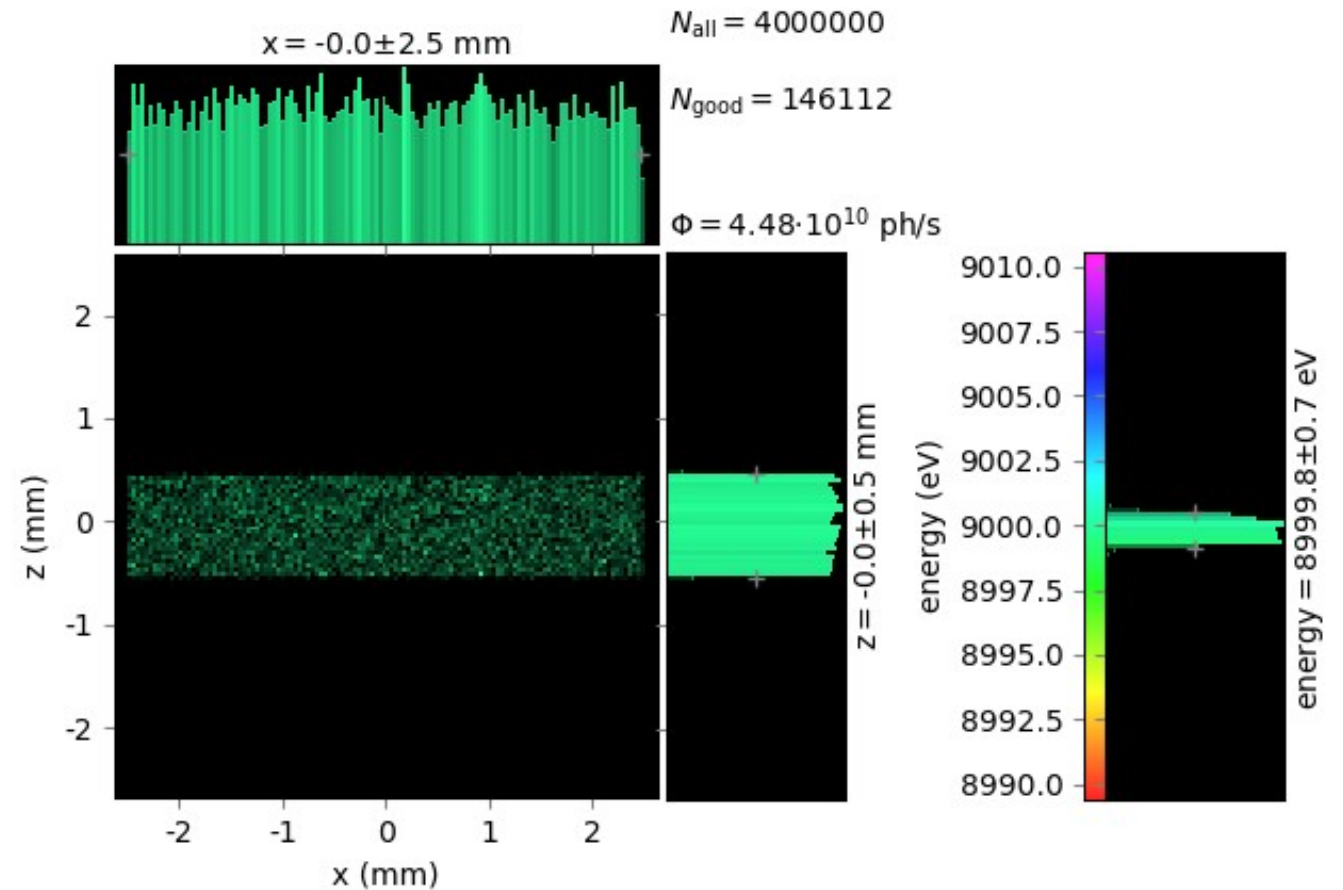
A bending magnet beamline for bulk XAFS

Ray tracing parameter:

- Bending magnet 1.2 Tesla
- Sample 60 m from source
- Collimating mirror (toroid) at 37 m collects 2 cm of horizontal divergence
- Si 111 DCM at 38.5 m
- Final slit 1*5 mm² (v*h)
- Tuned to 9000 eV

Today (P65):

- 11 period U33
- Beamsize 0.5*1.5 mm² (v*h)
- Monochromatic flux $\sim 10^{12}$ s⁻¹



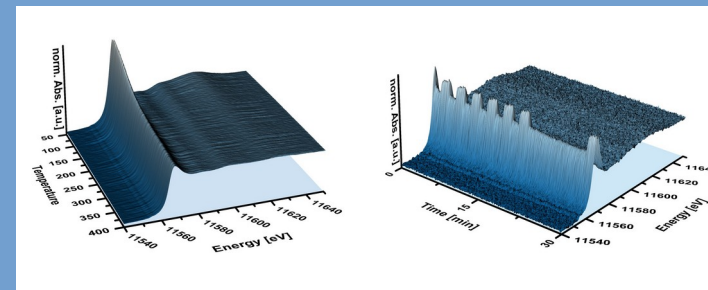
PETRA specific problem: Large radius => large distance of first optical element (Collimating mirror)

Quick scanning XAFS

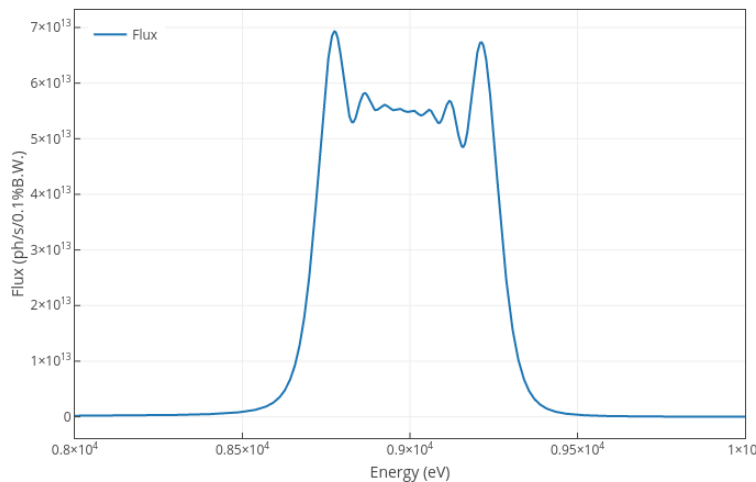
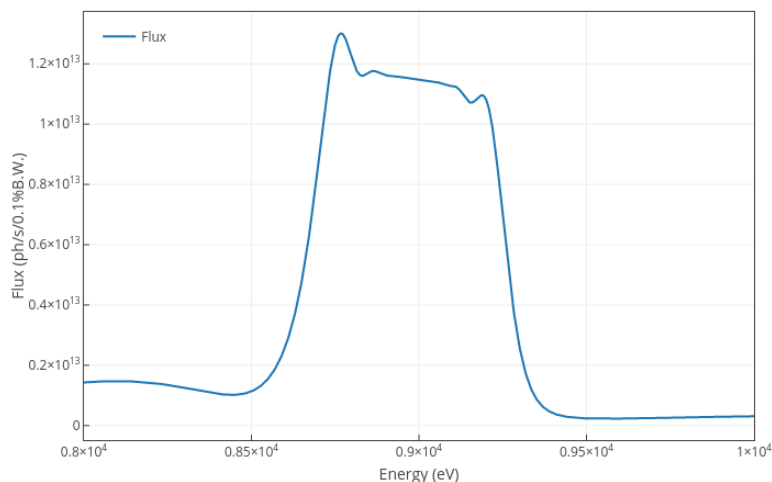
EXAFS with 100 Hz

Needs:

- Homogeneous beam
- Now spatial intensity fluctuations with energy
- High photon flux on the sample surface $> 10^{12} \text{ s}^{-1}$
- Fast scanning monochromator



Pt-L3 edge XANES during a temperature programmed reduction (left) and reducing/oxidizing cycles (right) of a Pt based catalyst. Data courtesy by Andreas Gänzler (KIT).



Flux through a pinhole (1*1 mm²), 80 m distance from source, tapered U33 undulator, 150 periods. PIII left, PIV right. FwhM ~ 500 eV

Calculations done with Spectra 11 (J. Synchrotron Radiation 8, 1221 (2001))

Beyond classical XAFS spectroscopy

High brilliance / Small focus

Spatial resolution and high flux density

Beam properties:

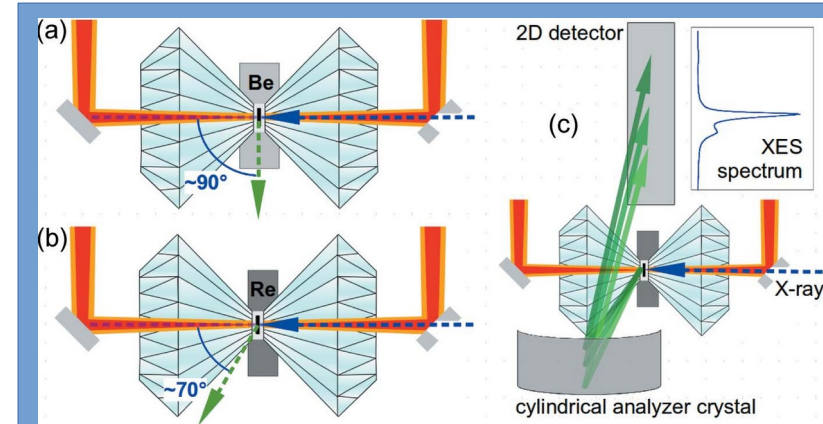
- Focused beam
- Monochromatic flux: $> 10^{12} \text{ s}^{-1}$
- Ideal source: Undulator

Methods:

- μ -XAFS
- XAFS-tomography

Applications:

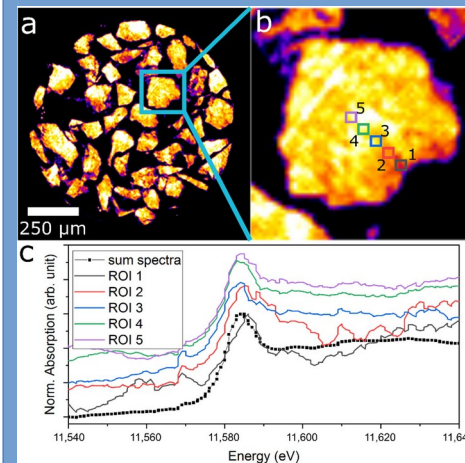
Catalysis, highly diluted samples, extreme conditions, grazing incidence XAFS



Laser heated Diamond Anvil Cell & Spectroscopy

spectroscopy (and diffraction) on laser-heated melts, heated spot $20 \mu\text{m}$, rapid measurements or pulsed heating & measurement

G. Spiekermann et al., J. Synchr. Rad. **27** (2020)



Catalyst sample in capillary measured at 553 K; (a) reconstructed slice, color-coding depicting the absorption intensity at 11,585 eV; (b) extracted single particle of the same slice with marked regions of interest; (c) XANES spectra extracted from each region of interest

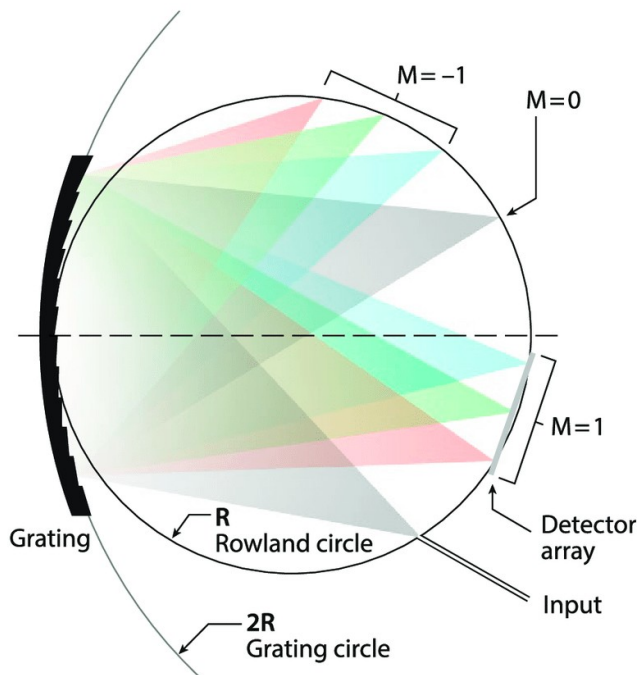
J. Becher et al., *Catalysts*, **11**, 459 (2021)

<https://doi.org/10.3390/catal11040459>

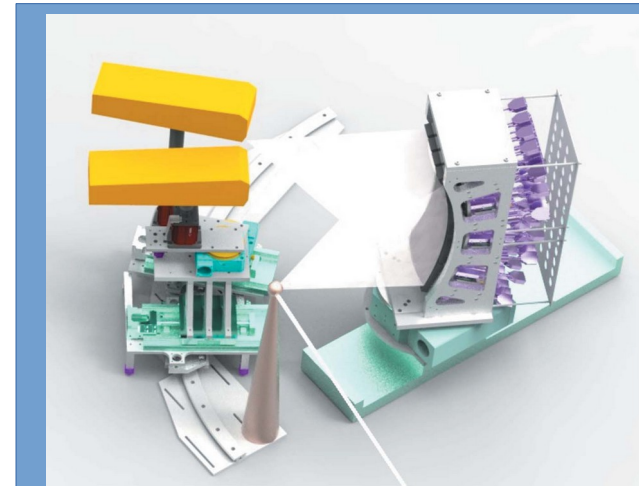
Spectrometers on the Rowland circle

High resolution emission spectroscopy and Co.

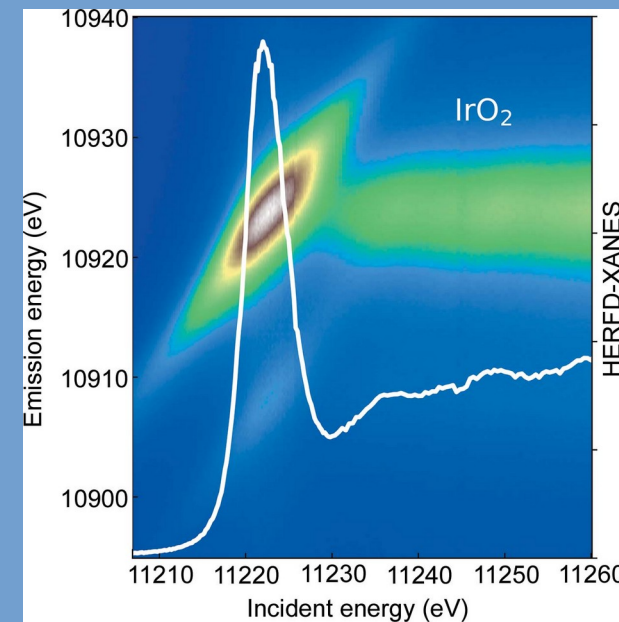
- Beamsizes limits energy resolution
- Photon hungry
- Applications profit from higher brilliance



From: Cataldo, Giuseppe (Thesis, 2015). *Development of ultracompact, high-sensitivity, space-based instrumentation for far-infrared and submillimeter astronomy.*



Mechanical drawing of the von Hamos spectrometer at P64 equipped with two detectors.



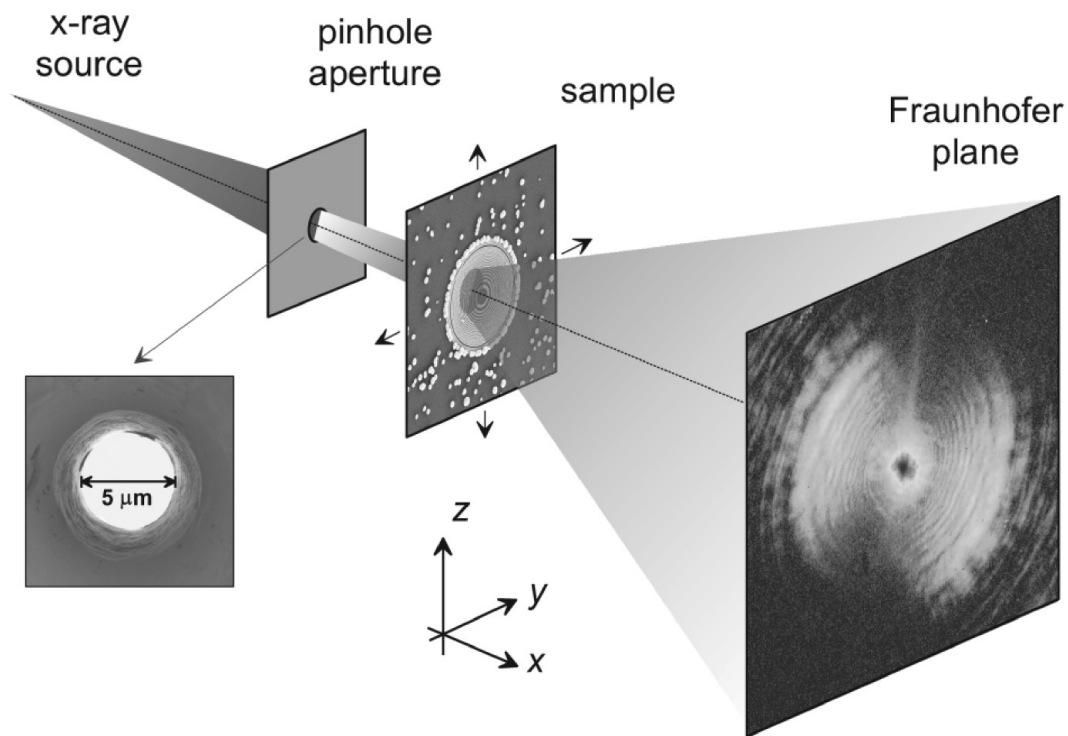
Ir L 3 -edge RXES plane and HERFD-XANES spectrum constructed from the plane by a cut at the maximum of the L 1 emission line.

A. Kalinko et al. *J. Synchrotron Rad.* **27**, 31–36 (2020)

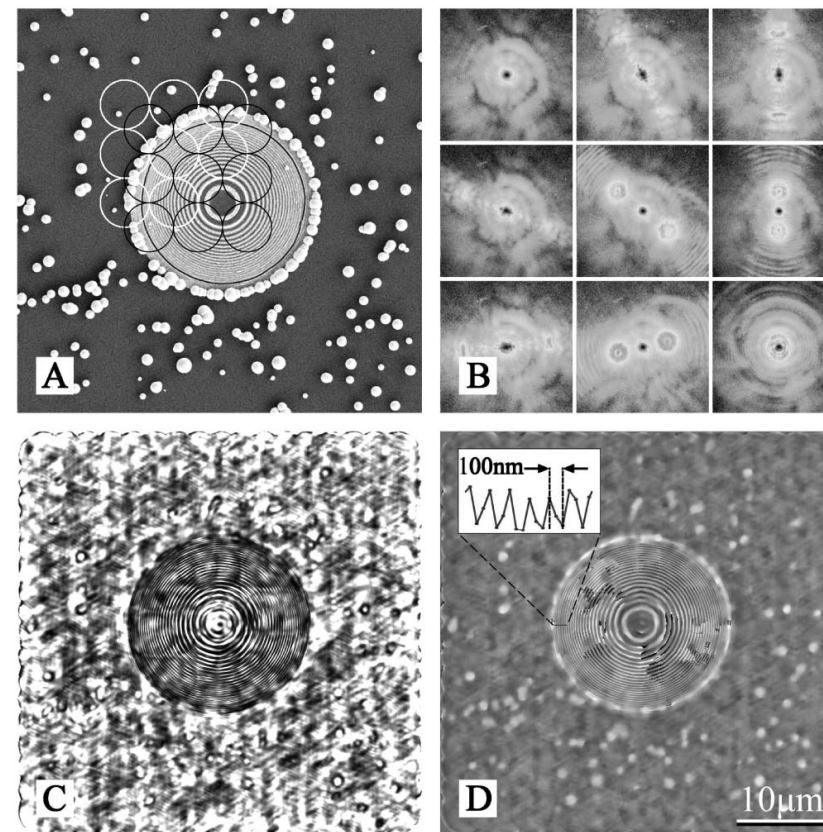
And finally coherence!

Ptychography

Hard-X-Ray Lensless Imaging of Extended Objects



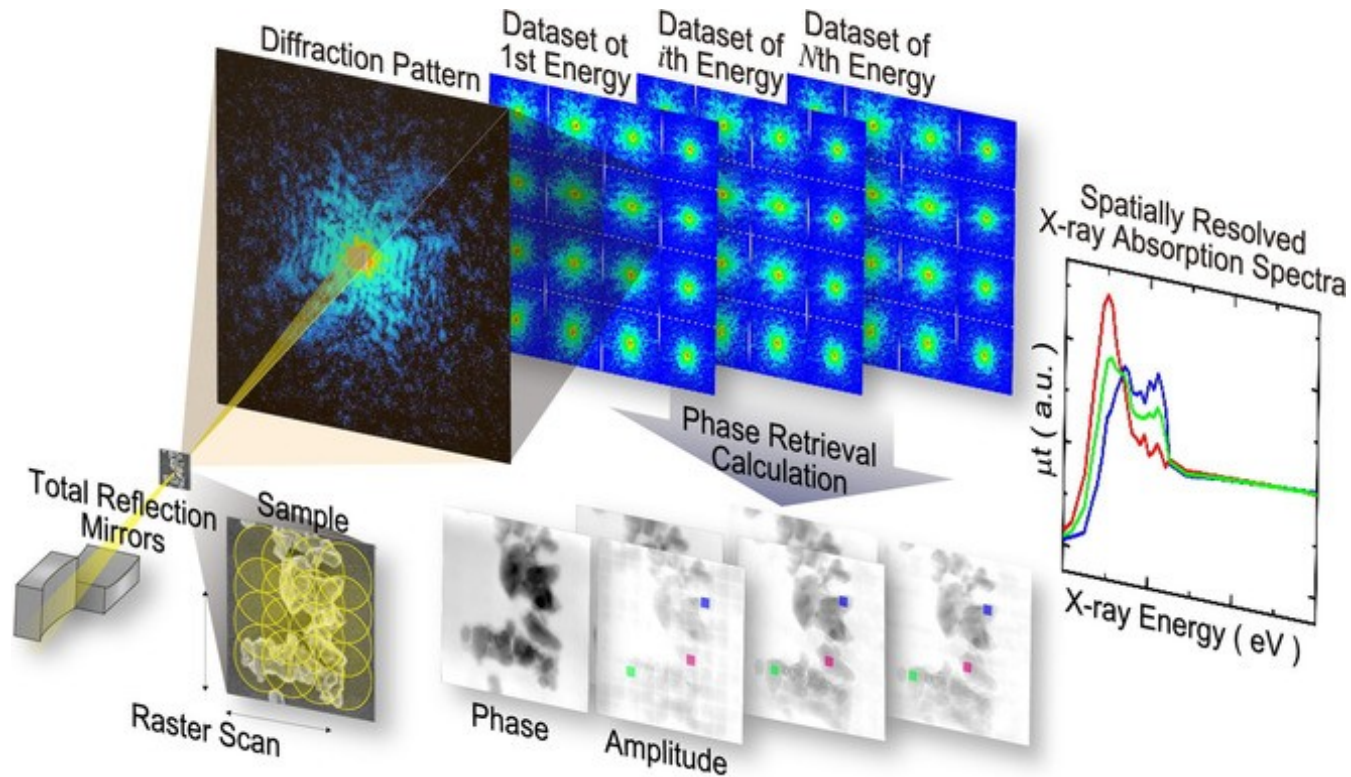
Schematic of the experimental setup for a shifting specimen coherent x-ray diffraction microscopy.



M. Rodenburg, A. C. Hurst, A. G. Cullis, B. R. Dobson, F. Pfeiffer, O. Bunk, C. David, K. Jefimovs, and I. Johnson, PRL 98, 034801 (2007)

XAFS-Ptychography

Adding a further “dimension”



X-ray spectro-ptychography or ptychographic-XAFS).

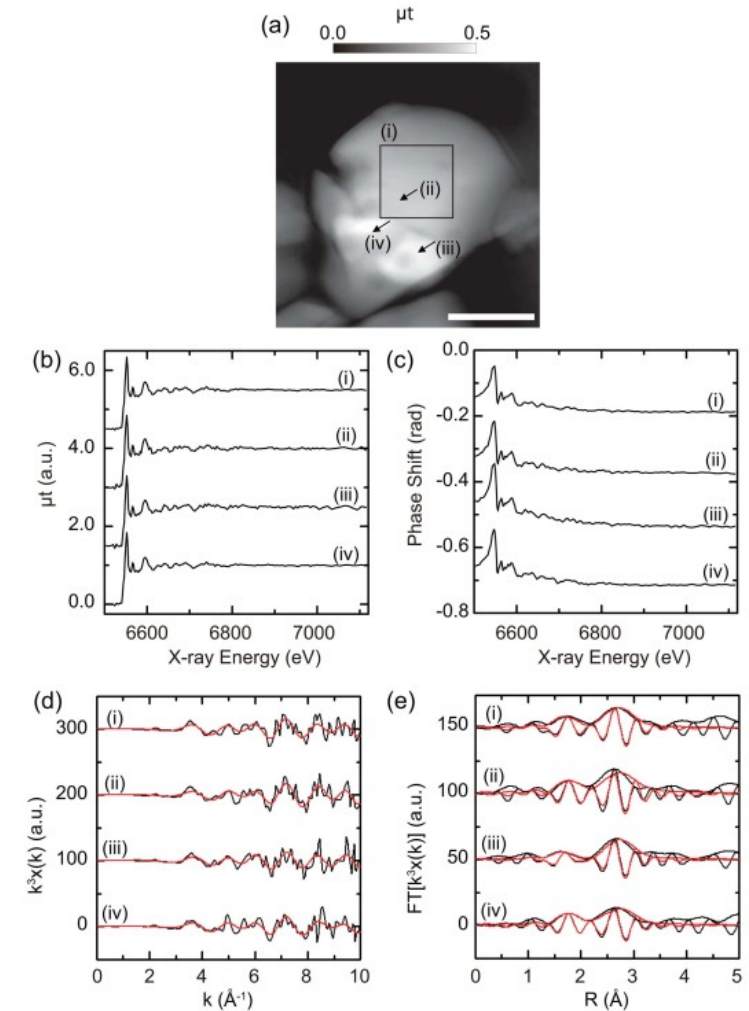
- Scanning of a focused coherent X-ray beam across the specimen at multiple X-ray energies.
- Phase and amplitude images are reconstructed from diffraction patterns by phase retrieval calculation.
- By analysing the energy dependence of the reconstructed images, spatially resolved X-ray absorption spectra are derived.

M. Hirose, N. Ishiguro, K. Shimomura, N. Burdet, H. Matsui, M. Tada and Y. Takahashi, *Angew. Chem. Int. Ed.*, **57(6)**, 1474-1479, (2017)
DOI: (10.1002/anie.201710798)

XAFS ptychography

Current limits

“Currently, the available flux of incident X-rays for the ptychography-XAFS method is **limited for the present synchrotron light source** since X-ray ptychography experiments **require highly coherent X-rays**. In **near-future synchrotron facilities**, the coherent X-ray flux will be **increased by a few orders of magnitude**, which will open up the possibility of visualization of spatio temporal chemical reactions and structural heterogeneities at an unprecedented high spatial resolution.”



Hirose et al., J. Synchrotron Rad. (2020). 27, 455–461 <https://doi.org/10.1107/S1600577519017004>

XAFS ptychography

Future perspectives

| | Mode | Undulator | Photon energy (keV) | Brilliance (ph/s/mm ² /mrad ² /0.1%bw) (Gauss) using Spectra | Brilliance (ph/s/mm ² /mrad ² /0.1%bw) (Wigner) using spectra | RMS photon source size (μm) (h x v) | RMS photon source divergence (μrad) (h x v) | FWHM beam size @ 100 m (μm) (h x v) | Coherence length @ 100 m (μm) (h x v) (GSM model) | Coherent fraction (GSM model) (%) (h x v) | Total Flux (ph/s) after DCM 38.5 m Si(111) | Coherent Flux (ph/s) after DCM 38.5 m Si(111) | Gain in coherent flux after DCM 38.5 m Si(111) comp. PIIJ | Total coherent fraction (GSM model) (%) |
|---------------------------------|-----------------|------------------|---------------------|---|--|-------------------------------------|---|-------------------------------------|---|---|--|---|---|---|
| PETRA III high beta | U33 / 2m | 2.4 (1st) | 6.72E+19 | | 160.64 x 9.06 | 14.33 x 12.11 | 4791 x 2760 | 85 x 1588 | 2.10 x 56.1 | 1.22E+13 | 1.46E+11 | 0.00 | 1.20 | |
| | | 6 (1st) | 1.12E+20 | | 160.54 x 7.14 | 10.99 x 7.87 | 4416 x 1767 | 42 x 635 | 1.12 x 39.0 | 2.81E+13 | 1.12E+11 | 0.00 | 0.40 | |
| | | 8 (1st) | 8.56E+19 | | 160.52 x 6.77 | 10.33 x 6.91 | 4493 x 1449 | 34 x 448 | 0.90 x 34.2 | 2.07E+13 | 6.42E+10 | 0.00 | 0.31 | |
| PETRA IV Brightness mode | U33 / 5m | 2.4 (1st) | 1.15E+22 | 1.38E+22 | 14.54 x 11.71 | 8.21 x 8.16 | 1789 x 1845 | 992 x 1775 | 54.7 x 74.4 | 6.49E+13 | 2.63E+13 | 179.98 | 40.60 | |
| | | 6 (1st) | 3.16E+22 | 3.69E+22 | 11.52 x 7.62 | 5.29 x 5.22 | 1153 x 1208 | 452 x 983 | 41.9 x 69.2 | 1.47E+14 | 4.25E+13 | 377.96 | 28.90 | |
| | | 8 (1st) | 2.87E+22 | 3.32E+22 | 10.93 x 6.71 | 4.63 x 4.55 | 1022 x 1022 | 342 x 787 | 36.7 x 67.2 | 1.08E+14 | 2.67E+13 | 415.71 | 24.70 | |
| PETRA IV Timing mode | U33 / 5m | 2.4 (1st) | 2.82E+21 | 3.69E+21 | 16.28 x 11.79 | 7.41 x 7.32 | 2059 x 2059 | 884 x 1846 | 45.1 x 72.6 | 2.60E+13 | 8.50E+12 | 58.07 | 32.70 | |
| | | 6 (1st) | 7.11E+21 | 8.69E+21 | 13.74 x 7.91 | 6.05 x 5.94 | 1344 x 1344 | 302 x 956 | 25.6 x 64.2 | 5.87E+13 | 9.63E+12 | 85.65 | 16.40 | |
| | | 8 (1st) | 6.28E+21 | 7.53E+21 | 13.24 x 7.02 | 5.31 x 5.19 | 1131 x 1188 | 204 x 693 | 20.8 x 56.6 | 4.36E+13 | 5.14E+12 | 80.17 | 11.80 | |

XAFS ptychography

Future perspectives

| | Mode | Undulator | Photon energy (keV) | Brilliance (ph/s/mm ² /mrad ² /0.1%bw) (Gauss) using Spectra | | Brilliance (ph/s/mm ² /mrad ² /0.1%bw) (Wigner) using spectra | | RMS photon source size (μm) (h x v) | | RMS photon source divergence (μrad) (h x v) | | FWHM beam size @ 100 m (μm) (h x v) | | Coherence length @ 100 m (μm) (h x v) (GSM model) | | Coherent fraction (GSM model) (%) (h x v) | | Total Flux (ph/s) after DCM 38.5 m Si(111) | | Coherent Flux (ph/s) after DCM 38.5 m Si(111) | | Gain in coherent flux after DCM 38.5 m Si(111) comp. PIIJ | | Total coherent fraction (GSM model) (%) | |
|---------------------------------|-----------------|------------------|---------------------|---|---------------|--|--------------|-------------------------------------|-------------|---|----------|-------------------------------------|--------|---|--|---|--|--|--|---|--|---|--|---|--|
| PETRA III high beta | U33 / 2m | 2.4 (1st) | 6.72E+19 | | 160.64 x 9.06 | 14.33 x 12.11 | 4791 x 2760 | 85 x 1588 | 2.10 x 56.1 | 1.22E+13 | 1.46E+11 | 0.00 | 1.20 | | | | | | | | | | | | |
| | | | 6 (1st) | 1.12E+20 | | 160.54 x 7.14 | 10.99 x 7.87 | 4416 x 1767 | 42 x 635 | 1.12 x 39.0 | 2.81E+13 | 1.12E+11 | 0.00 | 0.40 | | | | | | | | | | | |
| | | | 8 (1st) | 8.56E+19 | | 160.52 x 6.77 | 10.33 x 6.91 | 4493 x 1449 | 34 x 448 | 0.90 x 34.2 | 2.07E+13 | 6.42E+10 | 0.00 | 0.31 | | | | | | | | | | | |
| PETRA IV Brightness mode | U33 / 5m | 2.4 (1st) | 1.15E+22 | 1.38E+22 | 14.54 x 11.71 | 8.21 x 8.16 | 1789 x 1845 | 992 x 1775 | 54.7 x 74.4 | 6.49E+13 | 2.63E+13 | 179.98 | 40.60 | | | | | | | | | | | | |
| | | | 6 (1st) | 3.16E+22 | 3.69E+22 | 11.52 x 7.62 | 5.29 x 5.22 | 1153 x 1208 | 452 x 983 | 41.9 x 69.2 | 1.47E+14 | 4.25E+13 | 377.96 | 28.90 | | | | | | | | | | | |
| | | | 8 (1st) | 2.87E+22 | 3.32E+22 | 10.93 x 6.71 | 4.63 x 4.55 | 1022 x 1022 | 342 x 787 | 36.7 x 67.2 | 1.08E+14 | 2.67E+13 | 415.71 | 24.70 | | | | | | | | | | | |
| PETRA IV Timing mode | U33 / 5m | 2.4 (1st) | 2.82E+21 | 3.69E+21 | 16.28 x 11.79 | 7.41 x 7.32 | 2059 x 2059 | 884 x 1846 | 45.1 x 72.6 | 2.60E+13 | 8.50E+12 | 58.07 | 32.70 | | | | | | | | | | | | |
| | | | 6 (1st) | 7.11E+21 | 8.69E+21 | 13.74 x 7.91 | 6.05 x 5.94 | 1344 x 1344 | 302 x 956 | 25.6 x 64.2 | 5.87E+13 | 9.63E+12 | 85.65 | 16.40 | | | | | | | | | | | |
| | | | 8 (1st) | 6.28E+21 | 7.53E+21 | 13.24 x 7.02 | 5.31 x 5.19 | 1131 x 1188 | 204 x 693 | 20.8 x 56.6 | 4.36E+13 | 5.14E+12 | 80.17 | 11.80 | | | | | | | | | | | |

Summary

Summary

Challenges

- Classical XAFS spectroscopy does not gain from brilliance and/or coherence of 4th generation storage rings
- Beam inhomogeneities caused by diffraction will be amplified in more coherent beam
- The large flux density will increase problems with radiation damage and saturation of detectors (ionisation chambers)
- Superbends / short wigglers can be an attractive alternative at rings with smaller circumference and lower e⁻ energy than PETRA IV

Summary

Gains

- Methods that need high brilliance will gain from 4th generation sources
- This methods include μ -XAFs and XAFS-tomography
- Ptychographic XAFS is a very interesting method which will profit (be enabled) by the large fraction of coherent photons in the beam
- It will provide a 3-dimensional chemical mapping with high spatial resolution

Thank you

XAFS Journal Club Europe and Asia organised by Kiyotaka Asakura and Hitoshi Abe

Proposed talk by Prof. Takahashi about ptychographic-XAFS

Registration via:

https://docs.google.com/forms/d/e/1FAIpQLScyZVGEpGgFaAnMMk_ztaoasFrSx4nZ9fl1Ym_v8uVKiQZIIQ/viewform

Contact

DESY. Deutsches
Elektronen-Synchrotron

www.desy.de

Welter Edmund
FS-PETRA-S
edmund.welter@desy.de
+49 40 8998-4510

Planning new beamlines

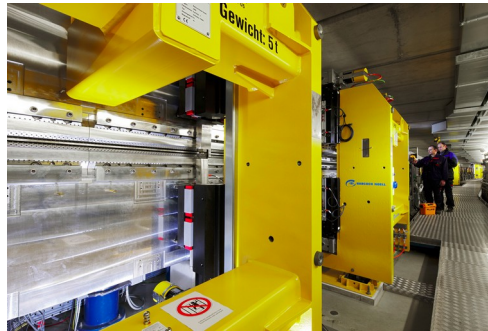
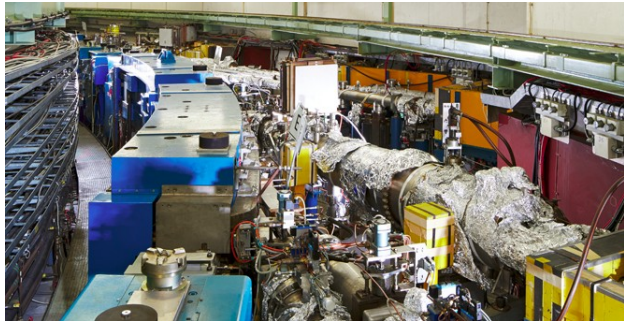
Ask users what they want to do in 5 – 10 years...

- Standard EXAFS (“large” beam, 1 min per scan, moderate flux density)
- Fast scanning XAFS (variable beamsize, 10 – 100 scans s⁻¹)
- High precision EXAFS ($k > 20 \text{ \AA}^{-1}$) (Usually “large” beam, highest possible spatial beam stability and homogeneity, moderate flux density)
- XAFS imaging with high spatial resolution (XAFS-tomography, μm^2 sized beam, high intensity/flux density)
- μ -XAFS $\ll 10 \mu\text{m}$ (μm^2 sized beam, high intensity/flux density)
-

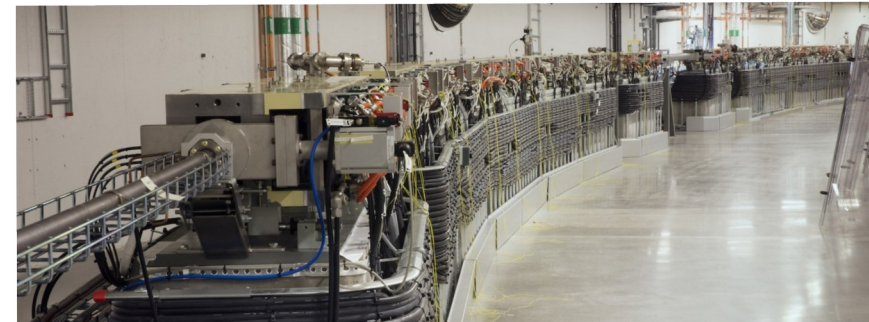
Home lab to synchrotron

The gap is getting larger

DORIS III bending magnets



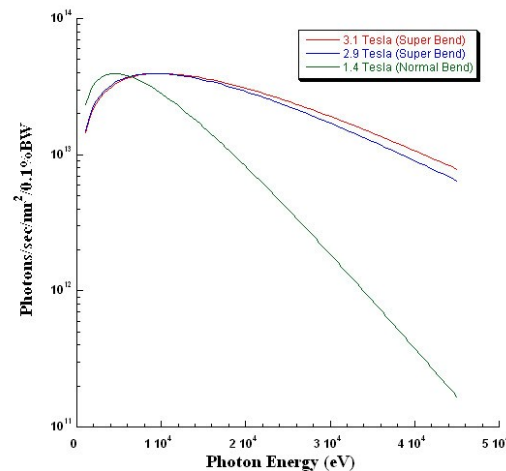
PETRA III undulators



MAX IV, the first operating 4th generation 3 GeV storage ring
Balder beamline, In vacuum wiggler (K=9), 38 periods, L = 50 mm



X-ray tube based bench-top XAFS devices



SuperBend at SLS (3 GeV, 3rd)
SuperXAS beamline